AWARD NUMBER: W81XWH-10-1-0275

TITLE: Androgenic Regulation of White Adipose Tissue-Prostate Cancer Interactions

PRINCIPAL INVESTIGATOR: Timothy C. Thompson, Ph.D.

CONTRACTING ORGANIZATION: University of Texas MD Anderson Cancer Center
Houston, TX 77030

REPORT DATE: August 2015

TYPE OF REPORT: Final

PREPARED FOR: U.S. Army Medical Research and Materiel Command
Fort Detrick, Maryland 21702-5012

REPORT DOCUMENTATION PAGE

Form Approved
OMB No. 0704-0188

1. REPORT DATE	2. REPORT TYPE	3. DATES COVERED
August 2015	Final	05/01/2010-05/31/2015

4. TITLE AND SUBTITLE

Androgenic Regulation of White Adipose Tissue-Prostate Cancer Interactions

5a. CONTRACT NUMBER
W81XWH-10-1-0275

5b. GRANT NUMBER

5c. PROGRAM ELEMENT NUMBER

6. AUTHOR(S)

Timothy C. Thompson, Ph.D.

E-Mail: timthomp@mdanderson.org

5d. PROJECT NUMBER

5e. TASK NUMBER

5f. WORK UNIT NUMBER

7. PERFORMING ORGANIZATION NAME(S) AND ADDRESS(ES)

University of Texas MD Anderson Cancer Center
Houston,Texas 77030

8. PERFORMING ORGANIZATION REPORT NUMBER

9. SPONSORING / MONITORING AGENCY NAME(S) AND ADDRESS(ES)

U.S. Army Medical Research and Materiel Command
Fort Detrick, Maryland 21702-5012

10. SPONSOR/MONITOR'S ACRONYM(S)

11. SPONSOR/MONITOR'S REPORT NUMBER(S)

12. DISTRIBUTION / AVAILABILITY STATEMENT

Approved for Public Release; Distribution Unlimited

13. SUPPLEMENTARY NOTES

14. ABSTRACT:

Glipr1 (mouse)/*GLIPR1* (human) is a direct p53 target gene that encodes a member of the pathogenesis-related protein family. This 28-kDa protein has a putative signal peptide sequence and a transmembrane domain suggesting extracellular functional activity. We have shown that Glipr1/GLIPR1 functions as a tumor suppressor through pro-apoptotic signaling in prostate cancer and potentially other malignancies. We recently discovered that recombinant Glipr1/GLIPR1 protein (rGlipr1/rGLIPR1) treatment results in growth arrest/apoptotic cell death in multiple prostate cancer cell lines in vitro. Further preclinical studies using PC-3 xenograft models demonstrated that rGLIPR1 suppressed PC-3 tumor growth when administered intratumorally or intraperitoneally. Although the direct growth suppressor/pro-apoptotic activities of Glipr1/GLIPR1 are now established, the physiological functions of GLIPR1 remain largely unknown. To further study Glipr1/GLIPR1 protein functions we generated mice harboring a targeted inactivation of the *Glipr1* gene. We discovered that the wet weight of *Glipr1* KO male white adipose tissue (WAT) was increased compare to the *Glipr*$^{+/+}$ male littermates (*Glipr1* WT). Based on these initial observations we pursued additional experiments. Overall, our preliminary data indicate that, in addition to direct growth suppressor/pro-apoptotic activities of Glipr1/GLIPR1 in prostate cancer cells, testosterone stimulated, prostate derived serum Glipr1/GLIPR1 is a hormone that can inhibit WAT function, including suppression of leptin secretion. Increased serum leptin levels may promote prostate cancer progression. We propose to study gene expression in the WAT and prostate tissues of *Glipr1* WT and *Glipr1* KO animals to characterize the genetic pathways that are affected by the presence or absence of Glipr1. We will also test the effects of surgical castration in the presence or absence of systemic rGlipr1 on adipocyte function and the development and growth of primary and metastatic prostate cancer using animal models. **Specific aims: Aim 1:** Characterize differentially expressed genes in WAT and prostatic tissues from *Glipr1* WT and *Glipr1* KO male mice; **Aim 2:** Study the effect of castration and rGlipr1 treatment alone and in combination on prostate cancer growth using human VCaP and PC-3 xenograft models; **Aim 3:** Study the effect of castration and rGlipr1 treatment alone and in combination on prostate cancer progression using an experimental metastases model.

15. SUBJECT TERMS

Prostate Cancer

16. SECURITY CLASSIFICATION OF:			17. LIMITATION OF ABSTRACT	18. NUMBER OF PAGES	19a. NAME OF RESPONSIBLE PERSON
a. REPORT	b. ABSTRACT	c. THIS PAGE			USAMRMC
Unclassified	Unclassified	Unclassified	Unclassified	24	19b. TELEPHONE NUMBER *(include area code)*

TABLE OF CONTENTS

FINAL REPORT

INTRODUCTION

Our proposed studies will test important parameters of the putative testosterone → prostate –| white adipose tissue (WAT) leptin axis and provide preclinical data for possible clinical trials. The information generated by our basic and preclinical experiments will reveal important new information regarding the molecular physiological activities of Glipr1/GLIPR1, a putative prostate derived hormone with direct and indirect systemic anti-tumor activities. The results of our experiments could also provide new predictive/prognostic serum markers for androgen ablation therapy in prostate cancer patients. Finally, our studies could provide critical preclinical data for development of systemic recombinant GLIPR1 protein (rGLIPR1) therapy to augment androgen ablation therapy for advanced prostate cancer. It is conceivable that our studies will lead to a new therapeutic approach that would involve administration of rGLIPR1 together with androgen ablation therapy. This would allow the replacement/augmentation of GLIPR1 that is suppressed by removal of testosterone. Administration of systemic rGLIPR1 would suppress WAT production of leptin and potentially other adipokines that promote prostate cancer progression. This potential new therapy may result in long-term control or possibly cures in patients with metastatic prostate cancer.

KEYWORDS

(castration-resistant prostate cancer)
(androgen deprivation therapy)
(androgen receptor)
(growth factors/chemokines)
(white adipose tissue)
(adipocyte stromal cells)
(castration)
(*Glipr1* WT and KO mice)
(macrophage)
(conditioned medium)
(GLIPR1-ΔTM protein therapy**)**
(WAT-associated macrophages)
(ventral prostate lobe)
(VCaP xenograft)
(orthotopic prostate tumor)
(systemic GLIPR1-ΔTM)
(acute, intermediate and chronic time points)
(microarray platform)
(gene expression)
(cytokine antibody array)

OVERALL PROJECT SUMMARY

Prostate cancer (PCa) cells are initially sensitive to hormonal manipulation, and androgen-deprivation therapy (ADT) generally reverses androgen receptor (AR)–dependent growth and proliferation. ADT is one of the main treatment modalities in the clinical management of PCa, but ADT is only palliative, and

PCa eventually progresses to an androgen-insensitive stage, i.e., castrate-resistant PCa (CRPC), after a median of 12–20 months. Progression to CRPC is a dynamic process that is incompletely understood as yet. Potential mechanisms contributing to the development of CRPC include selective growth of a preexisting hormone-insensitive population of cancer cells as a result of suppression by androgen ablation of the androgen-dependent cell population; activation of oncogenes; inactivation of tumor suppression genes; and interaction between cancer cells and tumor-associated stroma and tumor-associated macrophages. The object of this research project is to investigate the effect of castration on epididymal white adipose tissue (WAT), ventral prostate (VP) tissue, and adipose stromal cells (ASCs) from male *Glipr1*$^{+/+}$ (WT) and *Glipr1*$^{-/-}$(KO) mice. We are testing our hypothesis that the biologic activity of WAT is affected by castration and that although the acute effects of castration (e.g., GLIPR1 induction) may suppress cancer-promoting adipokines, long-term ADT results in monocyte infiltration and the generation of WAT-associated macrophages (WAMs). WAMs, in turn, produce cytokines and promote the growth and survival of growth factor–expressing ASCs, which enter the systemic circulation and promote PCa progression. An important note is that the prostate, an androgen target organ, is significantly affected by castration and also produces cytokines and cytokine receptors that may, in concert with WAT-derived cytokines, contribute to the progression of already established local tumors. We also hypothesize that Glipr1/GLIPR1 protein regulates castration-induced WAMs and ASCs. Our overarching hypothesis is that castration induces alterations in WAT that promote the development of CRPC.

Body – Statement of Work

Aim 1: Identify castration-affected and/or Glipr1-regulated genes in ventral prostate (VP) tissue, epididymal white adipose tissue (WAT), and adipocyte stromal cells (ASCs) using in vivo models.

1. Generate a sufficient number of *Glipr1* wild-type (WT) and *Glipr1* knockout (KO) 12-week-old male mice (1–6 months).
2. Perform the surgical castration experiment using the *Glipr1* WT and KO male mice, and collect VP, WAT, and ASCs on days 3, 14, and 35 after castration (6–9 months).
3. Isolate RNA and perform microarray analyses to characterize genes affected by castration in VP, WAT, and ASCs in *Glipr1* WT and KO male mice (9–12 months).

Aim 2: Study the interactions between ASCs isolated from *Glipr1* WT (ASCs-WT) and KO (ASCs-KO) male mice and human prostate cancer cell lines in vitro and in vivo.

1. Isolate, expand, and prepare a stock of frozen ASCs from *Glipr1* WT and KO male mice (6–12 months).
2. Determine the effect of ASCs on the cell growth rate of human prostate cancer cell lines in vitro (12-18 moths).
3. Determine the effect of ASCs conditioned media on the cell growth rate of human prostate cancer cell lines in vitro (12-18 moths).
4. Analyze and compare cytokine and growth factor profiles in conditioned media produced by ASCs (18-24 moths).

Aim 3: To test the response to surgical castration and systemic GLIPR1-ΔTM in vivo using VCaP xenograft model:

1. Generate orthotopic VCaP tumors in athymic nude male mice and determine the effect of surgical castration on the tumor growth and ASCs infiltration profiles at acute, intermediate and chronic time points.

2. Test the effects of systemic GLIPR1-ΔTM on orthotopic VCaP tumor growth and ASCs infiltration profiles ± surgical castration at acute (3d), intermediate (14d) and chronic time points (35d).

Research Results

Aim 1: Identify castration-affected and/or Glipr1-regulated genes in ventral prostate (VP) tissue, epididymal white adipose tissue (WAT), and adipocyte stromal cells (ASCs) using in vivo models.

1. Generate a sufficient number of *Glipr1* wild-type (WT) and *Glipr1* knockout (KO) 12-week-old male mice (1–6 months).
2. Perform the surgical castration experiment using the *Glipr1* WT and KO male mice, and collect VP, WAT, and ASCs on days 3, 14, and 35 after castration (6–9 months).
3. Isolate RNA and perform microarray analyses to characterize genes affected by castration in VP, WAT, and ASCs in *Glipr1* WT and KO male mice (9–12 months).

Animals and treatments. During the initial years of funding period, we generated *Glipr1*$^{+/+}$ (*Glipr1* WT) and *Glipr1*$^{-/-}$ (*Glipr1* KO) mice and randomly allocated to three subgroups of 5–10 mice each. One subgroup underwent sham surgery, and the other two, surgical castration. The sham-operated animals and half of the castrated ones then received a subcutaneously implanted empty pellet (EP) on their back, creating, respectively, control (sham + EP) and castrated + EP (Cx + EP) subgroups. The second half of the castrated animals received implanted testosterone pellets (TP), creating a Cx + TP subgroup. Thus, we established the following experimental groups and subgroups*:

Group 1, 3 days postoperatively: WT control – 3d; Cx + EP – 3d; and Cx + TP – 3d
Group 2, 14 days postoperatively: WT control – 14d; Cx + EP – 14d; and Cx + TP – 14d
Group 3, 35 days postoperatively: WT control – 35d; Cx + EP – 35d; and Cx + TP – 35d

Group 4, 3 days postoperatively: KO control – 3d; Cx + EP – 3d; and Cx + TP – 3d
Group 5, 14 days postoperatively: KO control – 14d; Cx + EP – 14d; and Cx + TP – 14d
Group 6, 35 days postoperatively: KO control – 35d; Cx + EP – 35d; and Cx + TP – 35d

*Key: control = sham-operated + empty pellet (EP); Cx + EP = castration + EP; and Cx + TP = castration + testosterone pellet (TP).

The mice were euthanized and the epididymal WAT pads were collected from each mouse, as were the anterior, ventral (VP), and dorsolateral lobes of the prostate, an androgen-dependent organ used as a control, and the wet weight (ww) of all those tissues was measured.

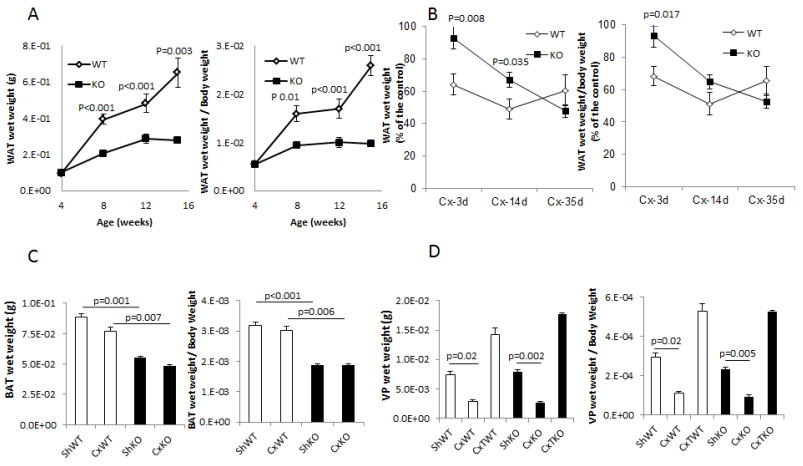

Fig. 1. A) Shows WAT weight. **B)** Shows WAT weight, % of the control, after castration. The response to castration in KO is delayed compared to WT. **C)** Brown adipose tissue weight. **D)** Ventral prostate weight.

Altered response of WAT to castration in *Glipr1* WT and KO mice. Analysis of epididymal WAT in *Glipr1* WT mice revealed that in the Cx + EP subgroups on days 3, 14, and 35 after castration, the WAT ww's

relative to those in the sham + EP control subgroups were 64 ± 6% ($P = 0.037$), 49 ± 6% ($P = 0.002$), and 60 ± 10% ($P = 0.020$), respectively.

In the Cx + TP WT subgroups, the WAT ww's were 83 ± 7%, 113 ± 7%, and 112 ± 15% of those of the sham + EP control subgroups on days 3, 14, and 35, respectively. The WAT ww:body weight ratios in the Cx + EP subgroups were 68 ± 6% (P = 0.030), 51 ± 7% (P = 0.001), and 65 ± 9% (P = 0.016) of those of the sham + EP controls on days 3, 14, and 35 after the surgery, respectively, whereas in the Cx + TP subgroups, the ratios were 81 ± 5%, 94 ± 4%, and 96 ± 11% of those in the controls.

Similar analysis of the WAT from the *Glipr1* KO mice revealed that the ww's in the Cx + EP subgroups were 93 ± 7%, 67 ± 5% (P < 0.001), and 48 ± 4% (P < 0.001) of those of the sham + EP controls on days 3, 14, and 35 days after the surgery, respectively.

In the Cx + TP group, the respective WAT ww's were 87 ± 6%, 138 ± 15% (P = 0.019), and 128 ± 7% (P = 0.012) of those of the controls. The WAT ww:body weight ratios in the Cx + EP subgroups were 93 ± 7%, 65 ± 4% (P < 0.001), and 53 ± 4% (P < 0.001) of those of the sham + EP control subgroups, respectively, on days 3, 14, and 35 after the surgery. In the Cx + TP group, those ratios relative to the control subgroups were 82 ± 6% (P = 0.040), 126 ± 11% (P = 0.041), and 127 ± 8% (P = 0.018), respectively.

Together, these results indicate that in the WAT from *Glipr1* KO mice, the response to castration is delayed relative to that in the WAT from the *Glipr1* WT mice. Further, the differences in WAT ww in the Cx + EP subgroups of the *Glipr1* WT and KO mice, expressed as percentages of that in the sham surgery + EP control subgroups, were statistically significant on days 3 (P = 0.008) and 14 (P = 0.035) after the surgical procedures (**Fig. 1**). Also, testosterone supplementation after surgical castration (i.e., Cx + TP) offset the effect of castration alone (i.e., Cx + EP) on days 14 and 35 days after castration. Further, testosterone caused a statistically significant increase in WAT ww's in *Glipr1* KO Cx + TP subgroups on days 14 and 35 after the surgery (**Fig. 1**).

Identification of genes in epididymal WAT that are altered by castration. As noted in the Methods, we used an Illumina microarray chip set to detect genes in the WAT whose expression was affected by castration in the *Glipr1* WT and KO Cx + EP and Cx + TP subgroups by postoperative day 14.

We considered only the genes that were up-regulated to at least twice their initial level of expression or down-regulated to half or less of their initial level of expression. We detected 40 up-regulated and 111 down-regulated genes in the WAT from the *Glipr1* WT Cx + EP subgroup and 389 up-regulated and 75 down-regulated genes in the Cx + TP subgroup. In the WAT from the *Glipr1* KO mice, we detected 126 up-regulated and 96 down-regulated genes in the Cx + EP subgroup and 548 up-regulated and 389 down-regulated genes in the Cx + TP subgroup. The most up-regulated and down-regulated genes in the experimental subgroups are listed in **Tables 1 and 2**.

Next, we analyzed genes that were expressed differently in the WAT from the *Glipr1* KO sham + EP subgroup than they were in that from the *Glipr1* WT sham + EP subgroup. We found 54 genes that were overexpressed and 62 genes that had reduced expression in *Glipr1* KO WAT relative to their expression in *Glipr1* WT WAT (**Table 3**).

Table 1. Genes with altered expression in the *Glipr1* wild-type (WT) mice after castration

Genes **up-regulated** in the castration + EP group		
Symbol	Entrez Gene Name	Fold Change
LOC100129193	major urinary protein pseudogene	7.3
IGHG	immunoglobulin heavy chain (gamma polypeptide)	5.9
ALDOC	aldolase C, fructose-bisphosphate	4.9
IGHA1	immunoglobulin heavy constant alpha 1	4.7
SPP1	secreted phosphoprotein 1	4.5
CDH16	cadherin 16, KSP-cadherin	3.7
CXCL13	chemokine (C-X-C motif) ligand 13	3.4
ITIH4	inter-alpha (globulin) inhibitor H4 (plasma Kallikrein-sensitive glycoprotein)	3.2
CELSR2	cadherin, EGF LAG seven-pass G-type receptor 2 (flamingo homolog, Drosophila)	2.9
ST3GAL6	ST3 beta-galactoside alpha-2,3-sialyltransferase 6	2.8
Genes **down-regulated** in the castration + EP group		
Symbol	Entrez Gene Name	Fold Change
PRM1	protamine 1	–10.9
CUZD1	CUB and zona pellucida-like domains 1	–9.5
DEFB129	defensin, beta 129	–9.3
SLC38A5	solute carrier family 38, member 5	–7.7
LY6F	lymphocyte antigen 6 complex, locus F	–7.1
RNASE12	ribonuclease, RNase A family, 12 (non-active)	–6.4
HP	haptoglobin	–6.2
SPINT4	serine peptidase inhibitor, Kunitz type 4	–5.9
CES7	carboxylesterase 7	–5.8
CRISP3	cysteine-rich secretory protein 3	–5.3
Genes **up-regulated** in the castration + TP group		
Symbol	Entrez Gene Name	Fold Change
GPX5	glutathione peroxidase 5 (epididymal androgen-related protein)	13.6
SPAG11B	sperm associated antigen 11B	13.0
SPINT4	serine peptidase inhibitor, Kunitz type 4	12.7
IDO1	indoleamine 2,3-dioxygenase 1	11.5
DEFA-RS1	defensin, alpha, related sequence 1	11.4
PLAC8	placenta-specific 8	11.2
LCN5	lipocalin 5	10.6
LY6G5C	lymphocyte antigen 6 complex, locus G5C	10.2
CRYBA4	crystallin, beta A4	9.5
DEFB129	defensin, beta 129	9.0
Genes **up-regulated** in the castration + TP group		
Symbol	Entrez Gene Name	Fold Change
PRM1	protamine 1	–4.4
C10ORF10	chromosome 10 open reading frame 10	–3.3
MFNG	MFNG O-fucosylpeptide 3-beta-N-acetylglucosaminyltransferase	–3.2
ACAA1B	acetyl-Coenzyme A acyltransferase 1B	–3.1
NNAT	neuronatin	–3.1
C3ORF1	chromosome 3 open reading frame 1	–3.0
TMEM45B	transmembrane protein 45B	–3.0
RETNLA	resistin like alpha	–3.0
AQP7	aquaporin 7	–2.8
PCSK6	proprotein convertase subtilisin/kexin type 6	–2.8

EP, empty pellet; TP, testosterone pellet.

Table 2. Genes with altered expression in the *Glipr1* knockout (KO) mice after castration

Genes **up-regulated** in the castration + EP group

Symbol	Entrez Gene Name	Fold Change
MMP12	matrix metallopeptidase 12 (macrophage elastase)	16.9
GPNMB	glycoprotein (transmembrane) nmb	14.7
LOC100129193	major urinary protein pseudogene	12.8
SPP1	secreted phosphoprotein 1	9.9
SLC40A1	solute carrier family 40 (iron-regulated transporter), member 1	6.5
VSIG8	V-set and immunoglobulin domain containing 8	6.3
CLEC4D	C-type lectin domain family 4, member D	6.3
TREM2	triggering receptor expressed on myeloid cells 2	6.0
CLEC7A	C-type lectin domain family 7, member A	5.0
LAT2	linker for activation of T cells family, member 2	4.7

Genes **down-regulated** in the castration + EP group

Symbol	Entrez Gene Name	Fold Change
PRM1	protamine 1	–10.6
HP	haptoglobin	–6.2
TIMP4	TIMP metallopeptidase inhibitor 4	–5.1
SNCG	synuclein, gamma (breast cancer-specific protein 1)	–4.8
SLC6A13	solute carrier family 6 (neurotransmitter transporter, GABA), member 13	–4.1
C7	complement component 7	–4.1
HSD11B1	hydroxysteroid (11-beta) dehydrogenase 1	–4.0
NPR3	natriuretic peptide receptor C/guanylate cyclase C (atrionatriuretic peptide receptor C)	–3.9
LRG1	leucine-rich alpha-2-glycoprotein 1	–3.3
PTPLB	protein tyrosine phosphatase-like (proline instead of catalytic arginine), member b	–3.3

Genes **up-regulated** in the castration + TP group

Symbol	Entrez Gene Name	Fold Change
GPX5	glutathione peroxidase 5 (epididymal androgen-related protein)	145.4
LCN5	lipocalin 5	66.3
DEFA-RS1	defensin, alpha, related sequence 1	57.4
IDO1	indoleamine 2,3-dioxygenase 1	52.2
CES7	carboxylesterase 7	46.4
C4BP	complement component 4 binding protein	39.2
PI3	peptidase inhibitor 3, skin-derived	38.0
CRISP3	cysteine-rich secretory protein 3	28.9
DEFB4A	defensin, beta 4A	26.5
LY6G5C	lymphocyte antigen 6 complex, locus G5C	24.8

Genes **down-regulated** in the castration + TP group

Symbol	Entrez Gene Name	Fold Change
RETNLA	Resistin-like alpha	–10.7
NNAT	neuronatin	–10.6
SNCG	synuclein, gamma (breast cancer-specific protein 1)	–10.0
GSN	gelsolin	–7.6
ANGPTL4	angiopoietin-like 4	–6.3
ADRB3	adrenergic, beta-3-, receptor	–6.2
MTUS1	microtubule associated tumor suppressor 1	–6.2
AQP7	aquaporin 7	–5.6
GPR81	G protein-coupled receptor 81	–4.8
TIMP4	TIMP metallopeptidase inhibitor 4	–4.8

Table 3. Genes with altered expression in the *Glipr1* KO sham-operated subgroup identified during comparison with the *Glipr1* WT sham-operated subgroup

Up-regulated

Symbol	Entrez Gene Name	Fold Change
MGST1	microsomal glutathione S-transferase 1	23.7
ME1	malic enzyme 1, NADP(+)-dependent, cytosolic	20.6
FCER1G	Fc fragment of IgE, high affinity I, receptor for; gamma polypeptide	10.1
MTUS1	microtubule associated tumor suppressor 1	7.9
NNMT	nicotinamide N-methyltransferase	6.6
SNCG	synuclein, gamma (breast cancer-specific protein 1)	6.2
CAP1	CAP, adenylate cyclase-associated protein 1 (yeast)	5.7
SUPT16H	suppressor of Ty 16 homolog (S. cerevisiae)	4.9
CYP2F1	cytochrome P450, family 2, subfamily F, polypeptide 1	4.8
HBD	hemoglobin, delta	4.6

Down-regulated

Symbol	Entrez Gene Name	Fold Change
SPAG11B	sperm associated antigen 11B	–12.3
DEFB129	defensin, beta 129	–10.6
SPINT4	serine peptidase inhibitor, Kunitz type 4	–10.5
GPX5	glutathione peroxidase 5 (epididymal androgen-related protein)	–9.1
RPL29	ribosomal protein L29	–8.8
CES7	carboxylesterase 7	–8.3
NECAP2	NECAP endocytosis associated 2	–7.2
RNASE12	ribonuclease, RNase A family, 12 (non-active)	–6.5
PRKAG2	protein kinase, AMP-activated, gamma 2 non-catalytic subunit	–6.4
RNASE9	ribonuclease, RNase A family, 9 (non-active)	–5.5

Castration-induced chemokines in the WAT from *Glipr1* WT and KO mice. Further analysis of the gene-expression data we obtained revealed that castration induced an increase in a limited number of chemokines: *Cxcl13* (3.4-fold) and *Ccl5* (2.3-fold) in the *Glipr1* WT Cx + EP subgroup and *Cxcl14* (2.4-fold) in the Cx + TP subgroup. In the *Glipr1* KO mice, we detected increases in *Ccl4* (2.6-fold), *Ccl9* (2.1-fold), and *Ccl3l3* (2.1 fold) in the Cx + EP group and *Cxcl14* (3.3-fold) in the Cx + TP group.

In summary, surgical castration induced changes in the genome of epididymal WAT. We identified genes that were up-regulated and down-regulated in WAT from the Cx + EP and Cx + TP subgroups of both *Glipr1* WT and KO mice. We also identified the post-castration(cx) up-regulation of a limited number of genes coding for cytokines.

Aim 2: Study the interactions between ASCs isolated from *Glipr1* WT (ASCs-WT) and KO (ASCs-KO) male mice and human prostate cancer cell lines in vitro and in vivo.

1. Isolate, expand, and prepare a stock of frozen ASCs from *Glipr1* WT and KO male mice (6–12 months).
2. Determine the effect of ASCs on the cell growth rate of human prostate cancer cell lines in vitro (12-18 moths).
3. Determine the effect of ASCs conditioned media on the cell growth rate of human prostate cancer cell lines in vitro (12-18 moths).
4. Analyze and compare cytokine and growth factor profiles in conditioned media produced by ASCs (18-24 moths).

WAT 12-w WT	Cx	SD
cxcl5	102.4	48.5
ccl4	7.5	2.0
il10	6.9	3.4
ccl3	5.9	1.6
ccr5	5.4	3.2
ccr4	5.1	0.5
cxcl2	5.0	2.7
il1a	4.5	3.2
ccl8	4.5	0.1
ccr7	4.3	1.4
ccl5	4.2	1.2
xcl1	4.1	0.3
il6	3.1	0.5
ccl6	3.0	1.5
tnfsf14	2.9	0.0
ccl9	2.9	0.8
tnfa	2.5	0.3
mmp2	2.4	0.2
cxcl5	108.6	84.5
ccr4	23.9	1.0
il1a	12.3	0.0
ccr7	8.5	1.1
il6	7.4	1.3
cxcl2	7.0	0.9
il10	5.2	0.5
ccl3	3.9	0.6
cx3cr1	2.7	0.1
cxcr3	2.6	0.3
ccl4	2.2	0.4
il1b	2.0	0.1

Employing cDNA microarray, we found proliferin upregulated in ASC from castrated mice compared to shamed mice but much higher level in ASC from *Glipr1*$^{-/-}$ than ASC from *Glipr1*$^{+/+}$ male mice. Thus, concluding that the castrated *Glipr1*$^{-/-}$ ASC contained highest level of secreted proliferin (**Fig. 2**).

Proliferin (PLF) was originally described as a glycoprotein secreted by mouse embryonic placental tissue during active midgestation period (Linzer, Lee et al. 1985; Toft and Linzer 2000). PLF belongs to the prolactin/growth hormone/placental lactogen family of polypeptide hormones, which are primarily produced in the pituitary gland and the placenta in most species (Corbacho, Martinez De La Escalera et al. 2002; Yang, Qiao et al. 2012). PLF has been associated with angiogenesis in sarcomas, gliomas, progressive fibrosarcoma and many other malignancies (Kandel, Bossy-Wetzel et al. 1991; Peles, Lidar et al. 2004; Yang, Qiao et al. 2012). Yang et al. reported secretion of PLF and binding to the regulatory regions of the PLF is required for STAT5-induced mouse endothelial cell migration, invasion, and tubule formation. (Yang, Qiao et al. 2012).

We found that conditioned medium (CM) from ASCs of castrated (cx) *Glipr1* WT and KO mice had more profound effect on prostate cancer cell lines in human (**Fig. 3A and 3B**) and mice prostate cancer cell line (**Fig. 4A and 4B**) in the cell growth and tubule formation.

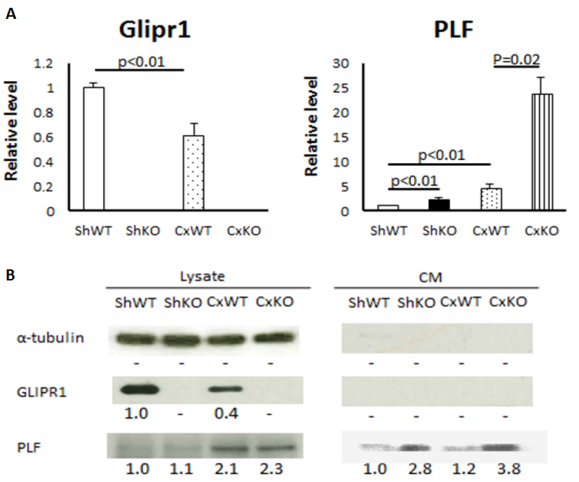

Fig. 2. (A) qRT-PCR with the primer specific for Glipr1 or PLF. Bar graph represents ratio relative to the amount of mRNA for each ASC to the shamed *Glipr1*$^{+/+}$ (ShWT). The amount of Glipr1 mRNA reduced approximately 40% after the castration. The amount of PLF mRNA in ASC subtypes increased in association with castration and *Glipr1* status. *Glipr1*$^{-/-}$ ASC (cxKO) showed the highest expression of PLF. **(B)** Expression of Glipr1 and PLF protein in ASC lysates and ASC-CM subtypes by western blotting. Expression of Glipr1 protein was reduced after castration in cxWT. PLF protein increased in association with castration and *Glipr1* status: cxKO showed the highest expression of PLF. α-tubulin was used as loading control.

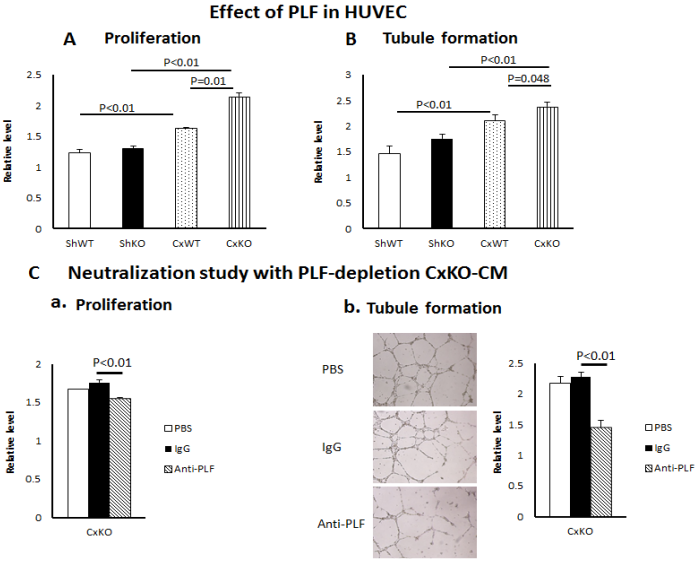

Fig. 3. (A) Effect of ASC-CM on HUVEC proliferation. CM collected from the cell sources indicated under columns was added to HUVEC. The number of living cells were measured using MTS assay. **(B)** Effect of ASC-CM on HUVEC tubule formation measured after 16–24 h. **(C)** ASC-CM pretreatment with PLF antibody decreased HUVEC proliferation (a) and tubule formation (b) stimulated by ASC-CM from castrated *Glipr1*$^{-/-}$ (CxKO) mice compared with ASC-CM treated with PBS or normal goat IgG. Images of the tubules formed were captured by phase contrast microscopy. The tubule lengths in each well were measured in 5 low-power fields. Bar graphs represent value or tubule length ratio relative to those in cells treated with serum free medium. Bars; SE.

Highest cell growth and tubule formation was attributed by ASC-CM from castrated *Glipr1* KO mice. Thus, our data indicated that surgical castration enhanced PLF (PLF-1 and PLF-2) secretion in ASC and higher level of secreted PLF was found in mice that do not have tumor suppressor *Glipr1*. Growth promoting effect of proliferin was confirmed by application of PLF antibody. PLF antibody neutralized the effect of PLF in the conditioned medium, blocking the cell growth, invasion and tubule formation of the cell lines (**Fig. 3C and Fig. 4C**). To our knowledge, this is the first report of surgical castration increasing secretion of trophic angiogenic factors such as PLF from ASC and this increase is exaggerated in absence of *Glipr1*. In summary our data indicate that castration promote CRPC condition by releasing factors that promote cell growth and angiogenesis such as PLF in ASC from the WAT, and release of these factors are increased in the absence of tumor suppressor genes such as *GLIPR 1*.

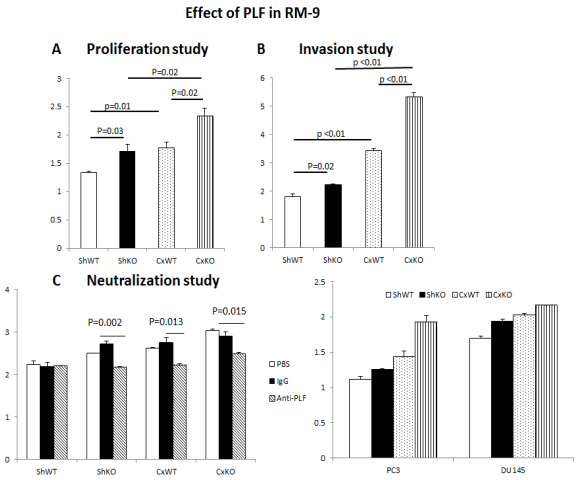

Fig. 4. (A) Effect of ASC-CM on mouse prostate cancer cell (RM-9) proliferation. CM collected from the cell sources indicated under columns was added to RM-9. The number of living cell measured using MTS assay. **(B)** Effect of ASC-CM on RM-9 invasion. RM-9 invasion was assayed as describe above. **(C)** Pre-treatment with PLF antibody decreased RM-9 proliferation. Each ASC-CM was either treated with PBS, normal goat IgG or anti-PLF antibody.

Aim 3: To test the response to surgical castration and systemic GLIPR1-ΔTM in vivo using VCaP xenograft model.

1. Generate orthotopic VCaP tumors in athymic nude male mice and determine the effect of surgical castration on the tumor growth and ASCs infiltration profiles at acute, intermediate and chronic time points.
2. Test the effects of systemic GLIPR1-ΔTM on orthotopic VCaP tumor growth and ASCs infiltration profiles ± surgical castration at acute (3d), intermediate (14d) and chronic time points (35d).

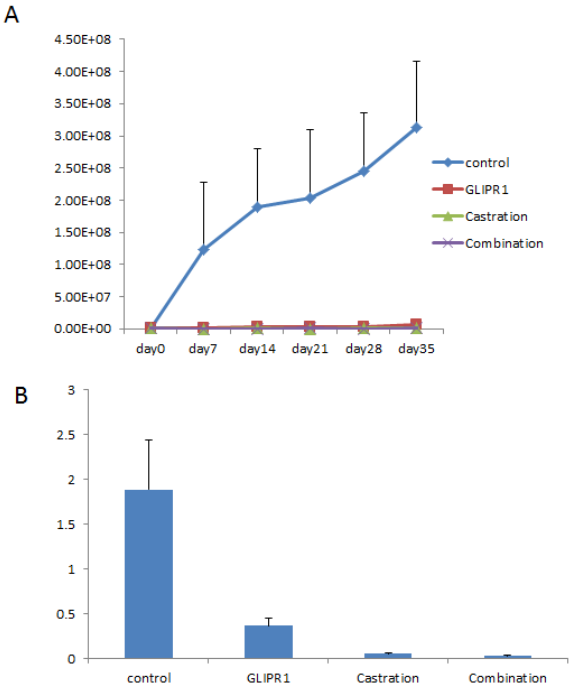

Fig. 5. A) VCaP-luc tumor growth measurement by IVIS. **B)** Tumor wet weight (g) after 35 days. Combination (GLIPR 1 –ΔTM protein + surgical castration)

We generated orthotopic VCaP (VCaP cells were previously transduced with the firefly luciferase gene in order to monitor tumor growth rate) tumors in four cohorts of athymic nude male mice by injecting $3x10^6$cells directly into dorsolateral prostate lobe. Two weeks later, on the same day, selected groups were subjected to surgical castration procedures. The mice were divided into the following treatment groups: control PBS, GLIPR1-ΔTM (20 µg of GLIPR1-ΔTM in 100µl of PBS i.p. for three consecutive days per week for 2 weeks) single treatment, castration alone, and GLIPR1-ΔTM+ castration (20 µg of GLIPR1-ΔTM in 100µl of PBS i.p. for three consecutive days per week for 2 weeks in addition to surgical castration). Each week, the tumor growth was measured by IVIS and after 35 days, the final tumor wet weight was measure (**Fig. 5a and 5b**).

Key Personnel

Principal Investigator: Timothy C. Thompson, Ph.D.; 713-792-9955; timthomp@mdanderson.org
Co-Investigators: Daniel Floryk, Ph.D.
Takahiro Hirayama, M.D.
Sanghee Park, B.S. Pharm.
Guang Yang, M.D., Ph.D.
Collaborator: Ju-Seog Lee, Ph.D.

KEY RESEARCH ACCOMPLISHMENTS

- The experimental groups were established, and biologic materials, including WAT, VP, and serum specimens, were collected as proposed. These samples will serve as a resource for future research in this area.
- We found that castration induces reductions of WAT wet weight and WAT wet weight:body weight ratios in *Glipr1* WT and *Glipr1* KO mice with different kinetics; the response is delayed in *Glipr1* KO WAT. Testosterone treatment offsets the effect of castration on WAT wet weight on days 14 and 35 after the surgery in both genotypes.
- Castration induces morphologic changes in adipocytes: cells become smaller and have a larger stromal compartment. The kinetics in the castration-induced WAT wet weight reduction differs between *Glipr1* WT and KO mice.
- Castration induces changes in the genome of WAT. We detected genes in which the up- or down-regulation was specific to the *Glipr1* WT or KO genotype.
- Castration induces secreted factors in adipose stromal cells that promote tumor growth and these factors are found in larger quantities in *Glipr1* KO mice.
- Highest levels of proliferin was found in adipose stromal cell conditioned medium of castrated mice but more so in the *Glipr1* KO mice compared to WT mice.
- The tumor promoting effect of proliferin was confirmed in vitro study conducted using HUVEC cells as well as mouse prostate cancer cells (RM-9).
- Proliferin promoted tumor cell growth as well as tubulin formation.
- Tumor cell growth and tubulin formation were neutralized by pre-treatment with proliferin antibody.
- GLIPR1-ΔTM protein treatment plus castration showed synergistic tumor suppressing effect in preclinical study done using VCaP tumor model.
- Further studies showed that chemokines that are potentially generated by WAT can promote resistance to docetaxel and potentially other chemotherapy agents. Importantly, GLIPR1-ΔTM treatment can overcome these effects. This important finding lays a foundation for application of GLIPR1-ΔTM therapy in future translational studies and clinical trials.
- Overall, our study confirmed that castration induced alteration in white adipose tissue microenvironment by secreting factors that promote castration resistant prostate cancer. However, rGLIPR1-ΔTM protein suppressed the tumor promoting factors in the preclinical tumor model.

CONCLUSION

Results of this proposed study indicate that androgen deprivation therapy and GLIPR1 protein, or a combination of GLIPR1 protein with an anti-cytokine receptor antibody could potentially delay or block

progression of prostate cancer. In addition, the results indicate benefit of modification of existing forms of androgen deprivation therapy to improve outcomes by considering anti chemokine therapy.

PUBLICATIONS, ABSTRACTS, AND PRESENTATIONS

a. Floryk D, Kurosaka S, Tanimoto R, Yang G, Goltsov A, Park S, Thompson TC. Castration-induced changes in mouse epididymal white adipose tissue. Mol Cell Endocrinology 345(1-2): 58-67, 2011. PMID: 21782885. PMCID: PMC3867123.
b. Thompson et. al. GLIPR1-DTM synergizes with docetaxel in cell death and suppresses resistance to docetaxel in prostate cancer cells. Molecular cancer (accepted).
c. Hirayama T, Park S, Goltsov A, Yang G and Thompson TC. Prostate Tumor Cell Growth Induced by Proliferin Secreted from Castrated *Glipr1*$^{-/-}$ Adipocyte Stromal Cells. (In preparation.)

INVENTIONS, PATENTS AND LICENSES
None

REPORTABLE OUTCOMES:
None

OTHER ACHIEVEMENTS
None

REFERENCES
None

APPENDICES

a. Floryk D, Kurosaka S, Tanimoto R, Yang G, Goltsov A, Park S, Thompson TC. Castration-induced changes in mouse epididymal white adipose tissue. Mol Cell Endocrinology 345(1-2): 58-67, 2011. PMID: 21782885. PMCID: PMC3867123.

Molecular and Cellular Endocrinology 345 (2011) 58–67

Contents lists available at ScienceDirect

Molecular and Cellular Endocrinology

journal homepage: www.elsevier.com/locate/mce

Castration-induced changes in mouse epididymal white adipose tissue

Daniel Floryk, Shinji Kurosaka, Ryuta Tanimoto, Guang Yang, Alexei Goltsov, Sanghee Park, Timothy C. Thompson *

Department of Genitourinary Medical Oncology – Research, The University of Texas MD Anderson Cancer Center, Houston, TX, USA

ARTICLE INFO

Article history:
Received 2 June 2011
Accepted 5 July 2011
Available online 12 July 2011

Keywords:
Castration
Regular diet
High-fat diet
Epididymal white adipose tissue
C57BL/6J mouse

ABSTRACT

We analyzed the effects of castration on epididymal white adipose tissue (WAT) in C57BL/6J mice which were fed a regular or high-fat diet. Fourteen days following surgical castration profound effects on WAT tissue such as reductions in WAT wet weight and WAT/body weight ratio, induction of lipolysis and morphologic changes characterized by smaller adipocytes, and increased stromal cell compartment were documented in both dietary groups. Castrated animals had decreased serum leptin levels independent of diet but diet-dependent decreases in serum adiponectin and resistin. The castrated high-fat group had dramatically lower serum triglyceride levels. Immunohistochemical analysis revealed higher staining for smooth muscle actin, macrophage marker Mac-3, and Cxcl5 in the castrated than in the control mice in both dietary groups. We also detected increased fatty-acid synthase expression in the stromal compartment of WAT in the regular-diet group. Castration also reduces the expression of androgen receptor in WAT in the regular-diet group. We conclude that castration reduces tissue mass and affects biologic function of WAT in mice.

1. Introduction

White adipose tissue (WAT) is a loose connective tissue that is crucial in the regulation of whole-body fatty-acid homeostasis. WAT is composed of adipocytes and other cells found in the stromal-vascular fraction, including macrophages, fibroblasts, pericytes, blood cells, endothelial cells, poorly differentiated mesenchymal cells, and preadipocytes (Fruhbeck, 2008). This dynamic, multifunctional endocrine tissue can secrete a large number of biologically active molecules, collectively called adipokines, which include hormones, growth factors, enzymes, cytokines, complement factors, and matrix proteins. For most of these molecules, WAT also expresses receptors that mediate extensive cross-talk both locally and systemically in response to specific external stimuli or metabolic changes (Fruhbeck, 2008; Galic et al., 2010). There is also an increasing body of evidence that a specific fat depot, the epididymal fat pad, produces a locally acting factor responsible for maintaining spermatogenesis in rodents (Chu et al., 2010; Hansel, 2010).

Storage of excessive fatty acids in an expanded adipose tissue mass characterizes obesity, which has reached epidemic proportions in the United States, where 35.1% of adults are now classified as obese (Catenacci et al., 2009). This epidemic is especially problematic because obesity is closely associated with the development of insulin resistance in peripheral tissues, such as skeletal muscle, and in the liver; moreover, it is an independent risk factor for the development of type 2 diabetes mellitus as well as myocardial infarction, stroke, and certain cancers (Galic et al., 2010). In fact, a high body mass index (BMI) is associated with increased risk of several common and less-common malignances in a sex- and site-specific manner. An association has also been reported between obesity and metabolic syndrome and not only with increased risk for the development of cancer but also for the progression of certain types of cancer (Fair and Montgomery, 2009; Roberts et al., 2010).

Additionally, adipose tissue is a major site for inflammation because the visceral adipose tissue depot contains more macrophages and releases more inflammatory cytokines, such as monocyte chemotactin protein 1 (MCP1)/CCL2, plasminogen activator inhibitor 1, and interleukin (IL) 6, IL-8, and IL-10, than subcutaneous adipose tissue does. In turn, inflammation in adipose tissue further increases the risk of obesity-related diseases and may be associated with the progression of cancer and its consequent mortality (Tran and Kahn, 2010).

The metabolism of adipose tissue is known to be affected by gonadal steroids such as testosterone. For example, testosterone deficiency, which can be caused by hypogonadism, aging, central obesity, or androgen-deprivation therapy in patients with prostate cancer, is associated with insulin resistance, type-2 diabetes, the metabolic syndrome, and cardiovascular disease in general (Bain, 2010).

* Corresponding author. Address: Department of Genitourinary Medical Oncology – Research, Unit 18-3, The University of Texas MD Anderson Cancer Center, 1515 Holcombe Boulevard, Houston, TX 77030-4009, USA. Tel.: +1 713 792 9955; fax: +1 713 792 9956.
E-mail address: timthomp@mdanderson.org (T.C. Thompson).

0303-7207/$ - see front matter © 2011 Elsevier Ireland Ltd. All rights reserved.
doi:10.1016/j.mce.2011.07.011

In mouse models, it has been demonstrated that cells from WAT are recruited by experimentally induced tumors and promote cancer progression (Zhang et al., 2009). Also, although surgical castration of mice results in increased glucose uptake into adipose tissue (Tran and Kahn, 2010), the effect of testosterone deficiency on adipose tissue has not been studied extensively.

Therefore, we undertook this study to identify the sustained effects of castration on WAT in adult male mice. We used C57BL/6J mice, which are commonly used for studies involving a high-fat diet (HFD) (Collins et al., 2004). We used a regular-diet and HFD approaches to assess differences in the responses to castration as the result of WAT deposition adjacent to the epididymis.

Our study results describe the changes in tissue mass, morphologic characteristics, induction of lipolysis, expression of genes coding for cytokines, and serum concentrations of adipokines that occurred in the epididymal WAT of adult mice fed a regular diet or a HFD after surgical castration.

2. Materials and methods

2.1. Animals and treatments

C57BL/6J mice, 5 and 10 weeks old, were purchased from MD Anderson Cancer Center's Department of Experimental Radiation Oncology. Mice were housed under specific pathogen-free conditions in facilities accredited by the American Association for Accreditation of Laboratory Animal Care, and all experiments were conducted in accordance with the principles and procedures outlined in the NIH's *Guide for the Care and Use of Laboratory Animals*.

For 7 weeks before and during the 2-week course of the experiments, the 5-week-old mice ($n = 45$) were fed a HFD (D12492; Research Diets, Inc., New Brunswick, NJ) containing 60 kcal% fat, 20 kcal% carbohydrate, and 20 kcal% protein, whereas the 10-week-old mice ($n = 30$) were fed a regular diet (Purina Conventional Rodent Chow 5001, St. Louis, MO) for 2 weeks. When all the mice were 12 weeks old, those in each dietary group were randomly allocated to three subgroups ($n = 10$–15 mice each), one of which underwent sham surgery, and the other two, surgical castration. We analyzed two independent groups ($n = 30$ per group) of mice fed with a regular diet and combined data for further analysis.

For the surgeries, mice were anesthetized with 2–4% isoflurane. After the surgical site was shaved, an incision was made in the scrotum. In the sham-surgery group, the incision was then simply closed with sutures. For castration of the other two groups, the incision was made in the tunica of the first testicle, and the testis was pulled out and removed. The procedure was repeated on the contralateral side. The scrotal incisions were then closed with sutures. The sham-operated animals and half of the castrated ones then received a subcutaneously implanted empty pellet on their back, creating control and castrated + empty pellet (EP) groups, respectively. The second half of the castrated animals received implanted testosterone pellets, creating a castrated + testosterone pellet (TP) group. Both testosterone (25 mg testosterone, 21-days release time) and placebo pellets were purchased from Innovative Research of America (Sarasota, FL).

2.2. Blood and tissue sampling and processing

All mice from both dietary groups were euthanized by using the CO_2 inhalation method 2 weeks after having undergone the surgical and pellet-implantation procedures. Their body weight and length were recorded. Blood samples were collected from the posterior vena cava, allowed to clot overnight at 4 °C, and then centrifuged for 20 min at 2000*g*. The resulting serum was stored frozen at −80 °C.

Further, the epididymal WAT pads were collected from each mouse, as were the anterior, ventral, and dorsolateral lobes of the prostate, an androgen-dependent organ used as a control, and the wet weights of all those tissues were measured. WAT tissue was processed as follows: one half of WAT was snap-frozen in liquid nitrogen and stored at −80 °C for further analysis of protein expression and RNA extraction. The second half of WAT was fixed in paraformaldehyde, embedded in paraffin, and cut into 5-μm sections for subsequent histologic and immunohistochemical (IHC) analyses.

2.3. Histological analysis of WAT

The effects of castration on the size of adipocytes were quantitatively evaluated using images, acquired at 20× magnification, of hemotoxylin and eosin (H&E)–stained WAT sections. The analysis was performed with a Nikon Eclipse 90i image analysis system and the NIS-Elements AR software 3.0 (both from Nikon Instruments, Inc., Melville, NY). One hundred randomly selected adipocytes from each section were outlined using the manual function of the system, and the areas of individual adipocyte profiles were recorded. To analyze the size distribution of adipocytes, the histogram function in Excel (Microsoft Corporation, Redmont, WA) was used and graphs were created.

2.4. Western blotting

A portion of each WAT specimen was homogenized in ice-cold radioimmunoprecipitation assay buffer by using a battery-powered handheld homogenizer (Sigma–Aldrich, St. Louis, MO). The resulting suspension was then spun in a bench centrifuge at 16,000*g* for 10 min. The supernatant was collected and cleared by passage through a Vivaclear Mini clarifying filter (Sartorius Stedim Biotech, Aubagne, France). Protein concentration was measured by using a protein assay kit from Bio-Rad Laboratories (Hercules, CA). Conventional Western blotting was performed using the following primary antibodies to visualize proteins: hormone-sensitive lipase (Hsl), phospho-hormone-sensitive lipase ($pHsl^{Ser660}$), adipose triglyceride lipase (Atgl), and fatty acid synthase (Fasn) all from Cell Signaling Technology, Beverly, MA). Gapdh (Santa Cruz Biotechnology, Inc., Santa Cruz, CA) was used as a loading control. Images were quantified with UN-SCAN-IT gel software Version 6.1 (Silk Scientific, Inc., Orem, UT).

2.5. Enzyme-linked immunosorbent assay (ELISA)

Serum testosterone concentrations were measured by using an ELISA kit (Calbiotech, Spring Valley, CA) according to the manufacturer's instructions. Serum leptin, adiponectin, and resistin concentrations were measured by using an ELISA kit for a respective cytokine (R&D Systems, Inc., Minneapolis, MN) according to the manufacturer's instructions.

2.6. Measurement of serum glucose and triglyceride (TG) levels

Serum glucose levels were measured using a glucose (GO) assay kit (Sigma–Aldrich). The manufacturer's procedure was modified to minimize the use of serum: 1 μl of serum was mixed with 99 μl of distilled water, and 200 μl of assay reagent was added. The reaction mix in a 1.7-ml test tube was incubated for 30 min at 37 °C. The reaction was stopped with 200 μl of 6 M sulfuric acid, and then 100 μl of the reaction mix was transferred to a 96-well plate. Absorbance at 540 nm was read by using a conventional plate reader.

Serum TG levels were measured by using a triglyceride assay kit (Cayman Chemical Company, Ann Arbor, MI) according to the manufacturer's protocol.

2.7. Gene-expression analysis

Total RNA was isolated from frozen WAT specimens by using a standard extraction protocol with Trizol reagent (Invitrogen Corporation, Carlsbad, CA). An iScript™ cDNA Synthesis Kit from Bio-Rad was used to generate cDNA for further analysis by quantitative real-time polymerase chain reaction (qRT-PCR) testing with SYBR Green stain. We initially used a Mouse Chemokines & Receptors RT^2 Profiler PCR Array (SA Biosciences, Frederick, MD) to detect genes that were affected by castration in epididymal WAT. Genes that were up-regulated after castration were further analyzed by using primers from PrimerBank (Spandidos et al., 2010).

2.8. IHC analysis

IHC with primary antibodies to the stromal marker smooth muscle α-actin (Acta2; 1:1000 dilution, Sigma, cat# A5228), Cxcl5 (1:50, R&D Systems, cat# MAB433), the macrophage marker Mac-3 (1:50, BD Biosciences, Pharmingen, San Diego, CA, cat# 550292), Fasn (1:50;Cell Signaling Technology, cat# 3180), and androgen receptor Ar (1:50, Santa Cruz Biotechnology, cat# sc-816) was performed on paraffin-embedded sections of WAT pads using the Vectastain® ABC kit or ImmPRESS™ reagents (Vector Laboratories, Inc., Burlingame, CA) according to the manufacturer's instructions. Specificity of the IHC staining was verified by incubating WAT sections with nonspecific rabbit or mouse immunoglobulin G in place of the primary antibody.

Acta2 and Fasn immunostaining was evaluated quantitatively using the Nikon Eclipse 90i with the NIS-Elements AR software. Fifteen to 20 images from each immunostained section of the WAT pad were randomly acquired at 10× magnification. The area of stroma that stained positively for Acta2 was detected by using a pixel classifier that recognizes brown DAB staining; the results were recorded as the percentage of the Acta2-positive stroma among a total tissue area.

To quantify the Cxcl5 and Mac-3 IHC staining results, we used the manual function to count the stromal cells that stained positively on 20 images acquired randomly at 20× magnification and recorded the total number of positively labeled cells for each antibody.

2.9. Statistical analysis

Statistical analysis was performed in Microsoft Office Excel using two-tailed Student's *t* testing. The level of significance was set at $p < 0.05$. Values are expressed as mean ± SE.

3. Results

3.1. Castration induces changes in epididymal WAT

3.1.1. Regular-diet group

Analysis of epididymal WAT (20 mice in each group) wet weights revealed that in the castration + EP (castration) group of mice, the weight was lower than that in the sham-surgery control group (control) by 43% ($p < 0.001$), and in the castration + TP group, lower by 16% ($p = 0.01$) (Fig. 1A). The WAT wet weight/body weight ratios (Fig. 1B) were also lower, by 40% in the castration group and 22% in the castration + TP group, than in the control group ($p < 0.001$ for both comparisons). Together, these results indicate that testosterone supplementation after surgical castration partially offsets the effect of castration.

As expected, castration resulted in significantly reduced wet weights of all prostatic lobes (Fig. 1S, Supplementary data).To detect changes in the size of adipocytes, we evaluated the H&E-stained WAT sections from five mice in each group. The adipocytes in the castration group appeared smaller than those in the control and castration + TP groups did (Fig. 1C). Indeed, quantitative image analysis (Fig. 1D) revealed that the average area of the adipocytes was less in the castration group (1020 ± 116 μm^2; $p = 0.027$) than it was in the control (1522 ± 145 μm^2) and the castration + TP (1262 ± 67 μm^2) groups.

We also detected a change in the stroma that was characterized by more fibroblast-like stromal cells and macrophages in the WAT from the castrated group than there were in that from the control and castration + TP groups. Some small adipocytes were surrounded by stromal cells.

3.1.2. High-fat diet group

The HFD group had higher body weights, epididymal WAT wet weight/body weight ratios, and BMIs than the regular-diet group had (Fig. 2S, Supplementary data). The wet weights of the anterior, ventral, and dorsolateral prostate lobes, used as controls, are shown in Fig. 1S, Supplementary data.

Analysis of epididymal WAT (15 animals in each group) wet weight revealed that the castration group had reduced WAT wet weight by 53% ($p < 0.001$), and castration + TP group by18% ($p = 0.3$) compared to the control group (Fig. 2A). The castration group had reduced WAT wet weight/body weight ratio by 47% ($p < 0.001$), and the castration + TP group by 16% ($p = 0.28$) compared to the control group (Fig. 2B).

The analysis of H&E-stained WAT sections revealed that the size of adipocytes was reduced in the castration group compared to the control group (Fig. 2C). Reduced size of adipocytes in the castrated group was confirmed by the quantitative image analysis (Fig. 2D). The average area of the adipocytes was 2555 ± 257 μm^2 after castration compared to 4166 ± 228 μm^2 in the control group. The presence of testosterone (i.e., castration + TP group) ($p = 0.003$) prevented the reduction of the size of adipocytes only partially as the adipocyte average area was 3388 ± 268 μm^2.

Thus, castration induces statistically significant WAT weight and the WAT wet weight/body weight ratio reduction independently of diet, but testosterone treatment partially offsets the effect of castration on WAT wet weight. Castration also induces morphologic changes in adipocytes: cells become smaller and have a larger stromal compartment. In general, castration led to reduced adipocyte size, and this effect was reversed in part by testosterone in the regular-fat diet group but not in the HFD group.

3.2. Castration-induced lipolysis

We hypothesized that castration induces lipolysis in WAT on the basis of our observations of reduced WAT wet weight and reduced size of adipocytes. To validate this hypothesis, we performed Western blotting to analyze protein levels of Hsl, $pHsl^{Ser660}$, and Atgl in WAT from both dietary groups after experimental treatments. Western blotting (Fig. 3) revealed reduced $pHsl^{Ser660}$ levels by 46% ($n = 10$, $p = 0.004$) in WAT from the regular-diet group after castration. Atgl protein levels were reduced as well, but the reduction was not statistically significant. The protein level of Hsl was increased by 22% in the presence of testosterone; the $pHsl^{Ser660}$ levels and Atgl levels were similar to those detected in the castration group but without statistical significance.

In contrast, we detected an increase of almost 2.5 times the $pHsl^{Ser660}$ levels ($n = 5$, $p = 0.003$) and 40% increased Atgl protein levels ($n = 5$, $p = 0.006$) in WAT from the HFD group after

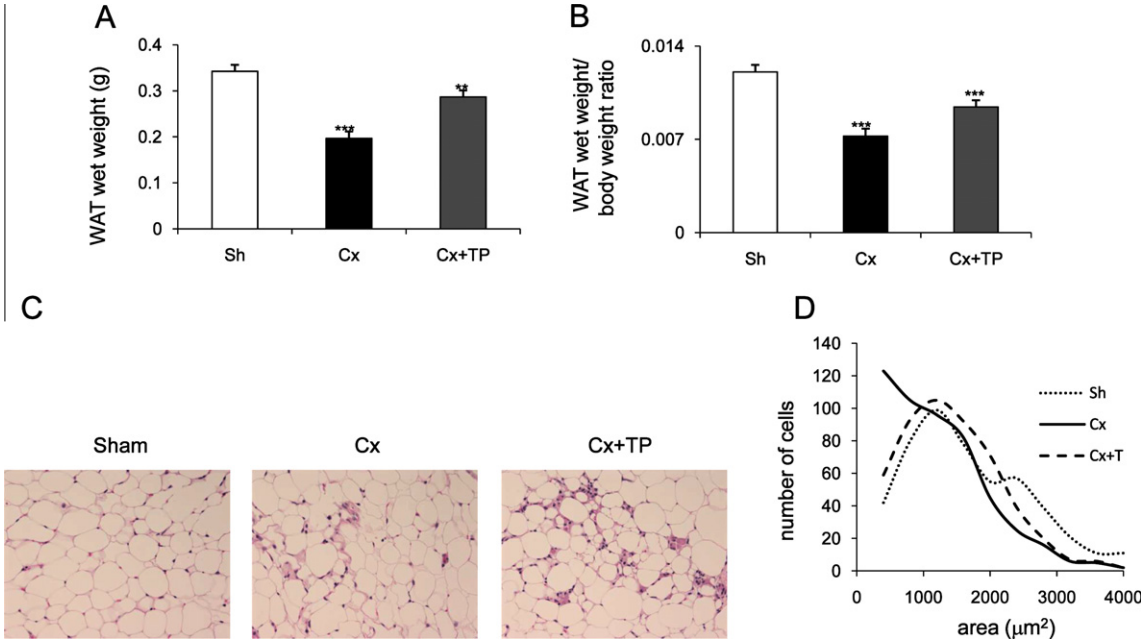

Fig. 1. The regular-diet group: (A) WAT wet weight, (B) WAT wet weight/body weight ratio, (C) hematoxylin and eosin staining of WAT, and (D) the adipocyte size distribution. (A) C57BL/6J mice fed regular diet were sham-operated, castrated, and castrated and treated with testosterone pellets as described in Section 2. At the end of the experiment, mice were euthanized and their WAT wet weights and body weights were recorded. Columns, WAT wet weight; bars, SE; $^{**}p < 0.01$; $^{***}p < 0.001$. (B) The WAT wet weight/body weight ratio was calculated. Columns, WAT wet weight/body weight ratio; bars, SE; $^{***}p < 0.001$. (C) Hematoxylin and eosin staining of WAT from sham-operated, castrated, and castrated + TP mice was performed as described in Section 2. Original magnification, 20×. (D) Line-graphs represent the adipocyte size distribution which was acquired by the image analyses. For each experimental group, 500 adipocytes were randomly selected from five specimens, and the areas of individual adipocytes were measured. Histogram function was used; bins were selected as 400 μm^2 increments.

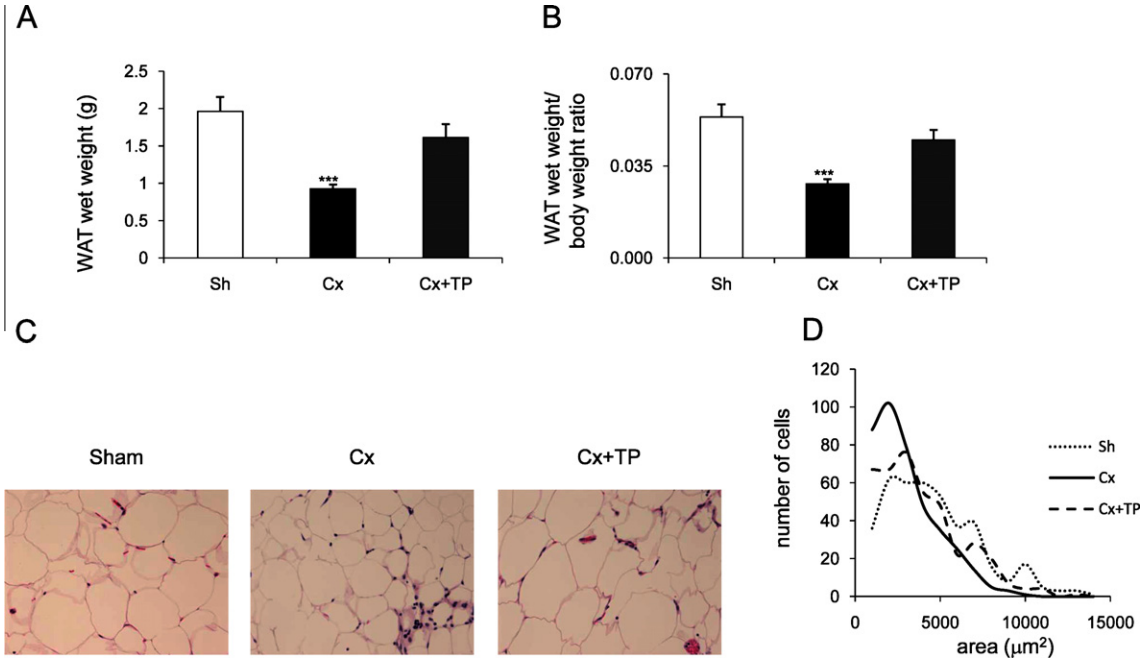

Fig. 2. The high-fat diet group: (A) WAT wet weight, (B) WAT wet weight/body weight ratio, (C) hematoxylin and eosin staining of WAT, and (D) the adipocyte size distribution. (A) C57BL/6J mice fed with high-fat diet were sham-operated, castrated, and castrated and treated with testosterone pellets as described in Section 2. At the end of the experiment, mice were euthanized and their WAT wet weights and body weights were recorded. Columns, WAT wet weight; bars, SE; $^{**}p < 0.01$; $^{***}p < 0.001$. (B) The WAT wet weight/body weight ratio was calculated. Columns, WAT wet weight/body weight ratio; bars, SE; $^{***}p < 0.001$. (C) Hematoxylin and eosin staining of WAT from sham-operated, castrated, and castrated + TP mice was performed as described in Section 2. Original magnification, 10×. (D) Line-graphs represent the adipocyte size distribution which was acquired by the image analyses. For each experimental group 500 adipocytes were randomly selected from five specimens and the areas of individual adipocytes were measured. Histogram function was used; bins were selected as 1000 μm^2 increments.

castration, suggesting that lipolysis is ongoing 14 days after castration. Differences detected in pHsl^{Ser660} and Atgl levels were offset by the presence of testosterone (Fig. 3).

Thus, it appears that castration-induced lipolysis in WAT of HFD-fed animals is more robust and/or sustained 14 days after castration than in animals fed a regular diet.

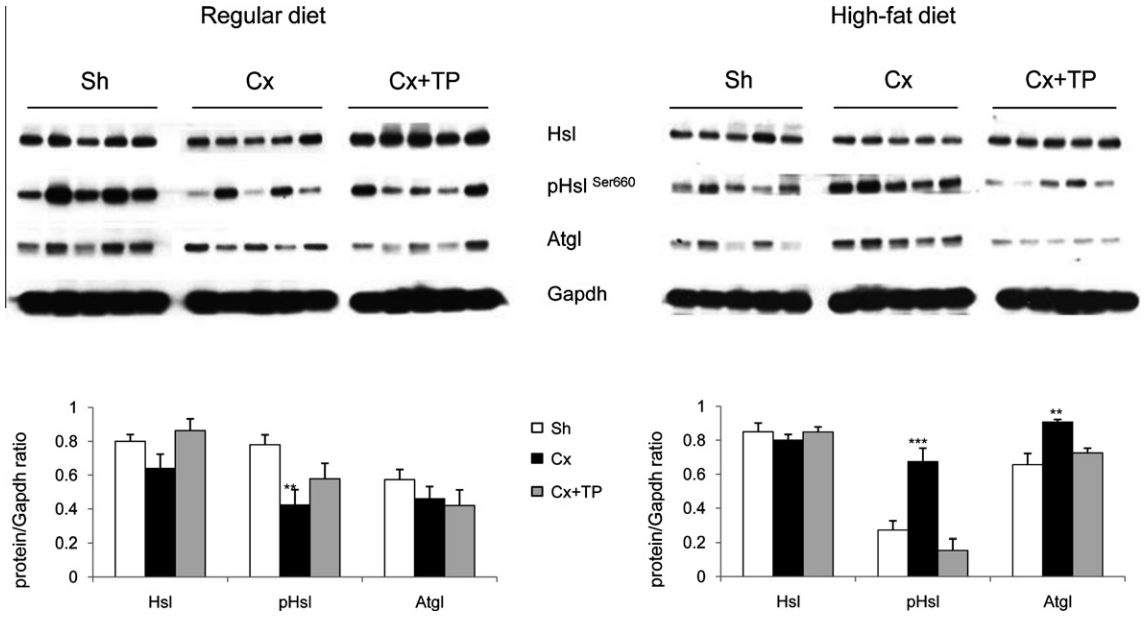

Fig. 3. Western blot analysis of hormone-sensitive lipase (Hsl), phosphorylated hormone sensitive lipase on serine 660 (pHsl^{Ser660}), adipose tissue triglyceride lipase (Atgl) protein levels in WAT from mice fed with regular diet and high-fat diet. Western blotting was performed as described in Section 2. Gapdh was used as a loading control. Images were quantified using UN-SCAN-IT gel 6.1 software to calculate protein/Gapdh ratio. Columns, protein/Gaphd ratio; bars, SE; $^{**}p < 0.01$; $^{***}p < 0.001$.

3.3. Serum adipokine levels

We further analyzed serum leptin, adiponectin, and resistin levels from mice from both dietary groups using commercial ELISA kits (Table 1). We detected reduced leptin levels in serum from the regular-diet group after castration by 72% ($n = 8$, $p < 0.001$) compared to the control group ($n = 8$). Castrated animals treated with TP also had reduced serum leptin levels by 46% ($n = 8$, $p = 0.007$) compared to the control group.

We detected increased adiponectin levels in serum from castrated mice by 13% ($n = 8$, $p = 0.0039$) compared to the control group. Castrated mice with TP had reduced serum adiponectin levels by 25% ($n = 8$, $p = 0.0004$) compared to the control group. Similarly, castration resulted in increased serum resistin levels by about 28% ($n = 8$, $p < 0.0001$) compared to the control group. Castrated mice with TP had serum resistin levels comparable with the control group.

The HFD group had reduced serum leptin levels after castration by 61% ($n = 8$, $p < 0.001$) compared to the control group ($n = 8$). Castrated animals treated with TP ($n = 8$) had serum leptin levels similar to the control group.

We did not detect castration-induced changes in serum adiponectin and resistin levels in castrated male mice compared to the controls.

Thus, mice fed a regular diet had reduced serum leptin and increased serum adiponectin and resistin levels after castration. The effect of testosterone was only partial as the serum leptin and adiponectin levels were lower compared to the control group. Castration had no effect on serum adiponectin and resistin levels in the HFD group.

3.4. Serum TG and glucose levels

We measured TG levels in serum collected from the control, castrated, and castrated + TP mice fed with a regular diet and HFD (Table 1). As expected, controls in the HFD group had higher serum TG levels than the controls in the regular-diet group had ($p = 0.03$). Castration of the regular-diet group resulted in a small but significant reduction in serum TG levels ($p = 0.018$) that was marginally offset by testosterone. However, castrated animals in the HFD group had three times lower serum TG levels than the control group had ($p = 0.002$). Castrated animals treated with testosterone had about two times lower serum TG levels than the control group had ($p = 0.013$), suggesting that testosterone did not offset the effect of castration.

We also measured serum glucose levels (Table 1). There were no differences in serum glucose levels in the regular-diet group. Control mice in the HFD group had significantly higher serum glu-

Table 1
Serum levels of adipokines, triglycerides (TG), and glucose.

	RD			HFD		
	Sh	Cx	Cx + TP	Sh	Cx	Cx + TP
Leptin (pg/ml)	2.5 ± 0.3	1.1 ± 0.2**	1.7 ± 0.3	24.3 ± 1.5	9.4 ± 0.9***	21.8 ± 2.0
Resistin (pg/ml)	22.4 ± 0.5	31.2 ± 1.1***	19.5 ± 1.0	30.6 ± 1.8	30.2 ± 2.2	28.7 ± 1.0
Adiponectin (μg/ml)	13.9 ± 0.1	15.6 ± 0.1**	10.4 ± 0.2***	13.6 ± 0.5	14.0 ± 0.3	12.9 ± 0.9
TG (mg/ml)	12.6 ± 0.8	10.4 ± 0.3*	11.2 ± 0.8	18.1 ± 2.5	6.3 ± 0.1**	9.3 ± 1.0*
Glucose (mg/ml)	2.3 ± 0.1	2.4 ± 0.1	2.4 ± 0.1	3.0 ± 0.1	3.6 ± 0.2*	3.4 ± 0.1*

Values are expressed as mean ± SE.
* $p < 0.05$.
** $p < 0.01$.
*** $p < 0.001$.

cose levels than the control mice from the regular-diet group had ($p = 0.004$). Castrated mice in the HFD group had increased serum glucose levels by 22% compared to the controls ($p = 0.027$). Increased serum glucose levels by about 14% were also detected in the castration + TP group compared to the controls ($p = 0.017$).

Thus, our data demonstrate that castration has a small but significant reduction of serum TG levels in the regular diet group and a dramatic reduction of serum TG in the HFD group. This effect was not offset by testosterone replacement in the HFD group. Serum glucose levels were affected only in the HFD group. Testosterone did not offset the castration effect.

3.5. Castration induces cytokines in epididymal WAT

It has been reported that in humans, visceral WAT generates and releases inflammatory cytokines, including CCL2, PAI-1, IL-6, IL-8, and IL-10, under specific conditions (Sengenes et al., 2007). We asked whether castration induces changes in the expression of genes coding for cytokines in epididymal WAT. qRT-PCR revealed that numerous cytokine genes are induced in WAT after castration. The most up-regulated genes were *Cxcl5*, *Cxcl2*, and *Il4* in WAT from the regular-diet group after castration (Table 2). Genes coding for *Cxcl5*, *Il1α*, and *Mmp2* were the most up-regulated in WAT from the HFD group after castration (Table 3). We also detected reduced leptin mRNA after castration (Tables 2 and 3). In both dietary groups, mRNA levels of genes coding for cytokines were lower compared to controls after testosterone treatment (Tables 2 and 3). We also compared mRNA levels of cytokines in control mice from the regular-diet and HFD groups. We detected increased expression of genes coding for *Cxcl1* (59.3 ± 31.7), *Ccl7* (22.5 ± 4.3), *Ccl2* (15.5 ± 5.3), *Cxcl2* (12.3 ± 3.1), *Tnf* (11.8 ± 2.6), and *Ccl3* (10.0 ± 0.7) in the HFD group numbers in brackets are fold ± SE.

Therefore, these experiments revealed that castration leads to changes in the expression of specific cytokine genes in epididymal WAT. *Cxcl5* was the most-induced cytokine in both dietary groups. Further, there is a set of cytokines which are produced at increased levels by WAT in the control HFD group compared to the control regular-diet group.

3.6. IHC staining of WAT

The H&E results suggested that castration induced morphologic changes in WAT associated with increased stromal compartment and macrophage infiltration (Figs. 1 and 2C). We performed IHC of paraffin-embedded WAT sections from the regular-diet (Fig. 4A) and HFD (Fig. 4B) groups. We used Acta2 as a stromal marker and Mac-3 as a macrophage marker. We also labeled sections with Cxcl5 and Fasn antibodies.

Fig. 4A shows stained sections and results of the quantitative analysis of WAT from mice on regular diet. Castration resulted in a significant increase of Acta2, Mac-3, and Cxcl5 protein expression. Testosterone offset castration-induced increase of Mac-3 and Cxcl5 proteins. Cxcl5 staining pattern suggests that Cxcl5 is most likely expressed by WAT macrophages.

We further hypothesized that increased presence of stromal cells in WAT is a result of the tissue regenerative process characterized by the presence of differentiating pre-adipocytes with the increased Fasn expression. IHC for Fasn confirmed that there is a subset of cells in WAT with increased Fasn staining. Increased Fasn staining was mostly localized to the stromal compartment of WAT after castration (Fig. 4A).

Fig. 4B shows stained sections and results of the quantitative analysis of WAT from the HFD group. Increased Acta2, Mac-3, and Cxcl5 proteins were detected, although the increases did not reach the level of statistical significance. Testosterone offset the castration-induced increase of Mac-3 and Cxcl5 proteins. We did not detect subset of WAT with increased Fasn staining in the HFD group (data not shown).

IHC staining for Fasn was confirmed by Western blotting (Fig. 3S, Supplementary data). We detected increased Fasn protein levels in WAT after castration in the regular-diet group compared to the control group (Fasn/Gapdh ratio was 1.15 vs 0.98, $n = 4$, $p = 0.008$). A slight increase of Fasn protein levels (Fasn/Gapdh ratio was 1.05 vs 0.98, $n = 4$) was not statistically significant in the castration + TP regular-diet group. We did not detect changes in Fasn protein levels in the HFD group.

Thus, IHC staining confirmed that castration-induced WAT morphologic changes are accompanied by changes in protein expression. We detected increased expression of Acta2, Mac-3, Cxcl5, and Fasn.

3.7. Effect of castration on the expression of androgen receptor Ar in WAT

Initially, we used ELISA to measure serum testosterone levels in samples ($n = 8$ per treatment group) from both diet groups. The analysis confirmed that castrated animals in both diet groups had background levels of serum testosterone; 0.04 ± 0.02 ng/ml or 0.05 ± 0.03 ng/ml in the regular-diet and the HFD group, respectively. We detected lower levels of serum testosterone in the control HFD group (0.26 ± 0.13 ng/ml; $p = 0.16$) than in the

Table 2
Changes in the cytokine expression in epididymal WAT 14 days after castration, regular diet.

			Cx		Cx + TP	
Gene	Gene ID	Official name	Fold	SE	Fold	SE
Cxcl5	20311	Chemokine (c-x-c motif) ligand 5	56.2	31.5	4.0	2.6
Cxcl2	20310	Chemokine (c-x-c motif) ligand 2	22.3	15.3	6.0	1.7
Il4	16189	Interleukin 4	15.9	7.6	4.1	2.4
Ccl3	20302	Chemokine (c-c motif) ligand 3	14.1	3.3	3.4	1.2
Xcl1	16963	Chemokine (c motif) ligand 1	9.7	5.2	1.7	0.0
Il10	16153	Interleukin 10	7.8	2.8	−1.2	1.3
Ccl2	20296	Chemokine (c-c motif) ligand 2	7.3	4.3	2.3	1.0
Tnf	21926	Tumor necrosis factor alpha	6.8	2.6	1.8	0.2
Il1a	16175	Interleukin 1 alpha	6.5	2.5	2.2	0.6
Ccl4	20303	Chemokine (c-c motif) ligand 4	6.3	1.4	−1.0	1.0
Cxcl1	14825	Chemokine (c-x-c motif) ligand 1	6.0	2.1	1.4	0.3
Il6	16193	Interleukin 6	5.5	1.6	1.8	0.4
Ccl7	20306	Chemokine (c-c motif) ligand 7	5.2	3.1	0.7	1.4
Mmp2	17390	Matrix metallopeptidase 2	4.3	0.5	2.1	0.5
Tnfrsf1a	21937	Tumor necrosis factor receptor superfamily, member 1a	3.1	0.5	1.6	0.4
Lep	16846	Leptin	−3.2	0.5	−0.1	1.2

Table 3
Changes in the cytokine expression in epididymal WAT 14 days after castration, high-fat diet.

			Cx		Cx + TP	
Gene	Gene ID	Official name	Fold	SE	Fold	SE
Cxcl5	20311	Chemokine (c-x-c motif) ligand 5	59.8	17.7	7.7	4.4
Il1a	16175	Interleukin 1 alpha	6.1	2.3	0.4	1.0
Mmp2	17390	Matrix metallopeptidase 2	6	0.8	1.0	1.3
Il12	16159	Interleukin 12	5.7	1.1	0.8	1.0
Il4	16189	Interleukin 4	5.4	1.6	−0.3	0.8
Ccl3	20302	Chemokine (c-c motif) ligand 3	4.8	1.6	3.7	1.1
Il10	16153	Interleukin 10	4.5	0.8	0.6	0.7
Tnf	21926	Tumor necrosis factor alpha	3.3	0.6	−0.1	0.8
Ccl4	20303	Chemokine (c-c motif) ligand 4	2.4	0.3	1.5	0.5
Lep	16846	Leptin	−4.4	1.7	−0.4	1.5

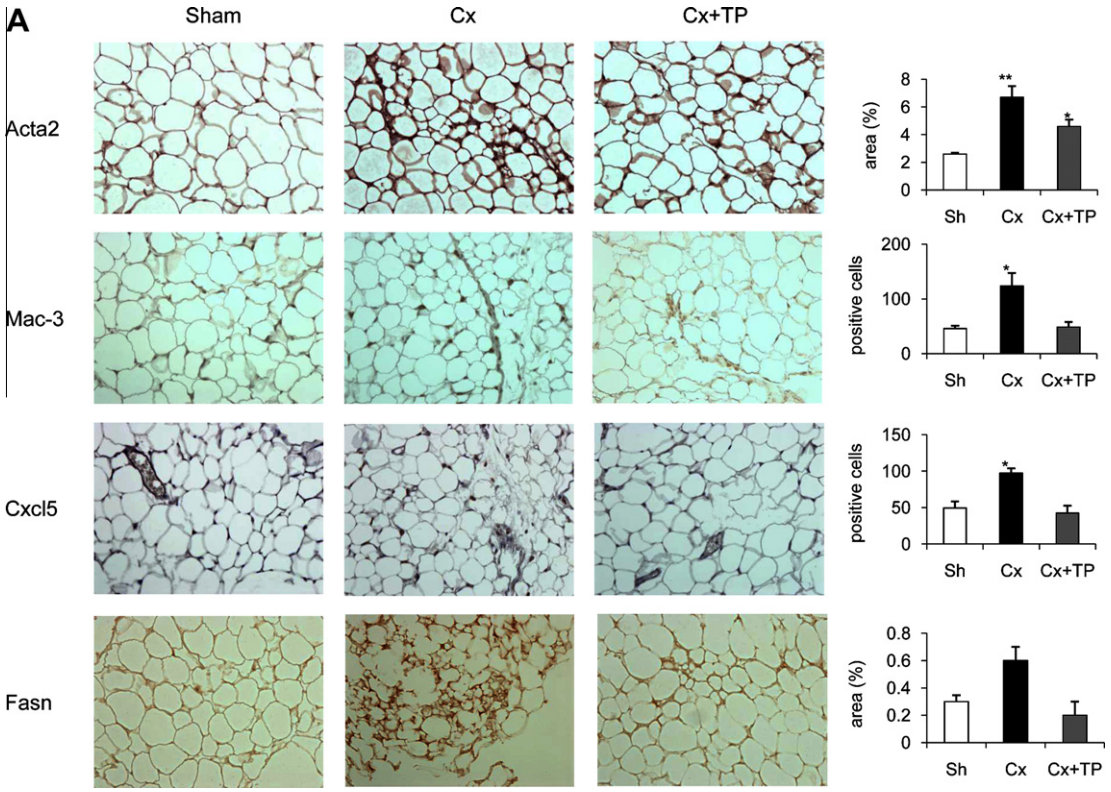

Fig. 4. Immunohistochemical (IHC) staining of paraffin-embedded WAT from mice fed a regular diet (A) or a high-fat diet (B). (A, B) Antibodies against smooth muscle actin (Acta2), Mac-3, Cxcl5, and Fasn were used as described in Section 2. Images were depicted at 20× magnification. Column graphs represent results from the semiquantitative analysis of the IHC images. Sh, sham-operated; Cx, castration; Cx + TP, castration + testosterone pellet. Bars, SE; $^{*}p < 0.05$; $^{**}p < 0.01$.

regular-diet group (1.65 ± 0.57 ng/ml). Implantation of testosterone pellets resulted in serum testosterone levels of 23.63 ± 0.81 ng/ml or 17.59 ± 0.70 ng/ml in the regular-diet and the HFD castration + TP group, respectively.

To assess the effect of castration on the expression of Ar, we performed qRT-PCR and IHC staining of WAT sections from both diet groups. In the regular-diet group, castration resulted in reduced Ar mRNA by 4.1 ± 0.9-fold. A similar decrease was detected in the castration + TP group (4.7 ± 1.4-fold). IHC staining (Fig. 5) revealed that nuclear Ar was undetectable in WAT from the castrated regular-diet group. Fewer cells stained for nuclear Ar in WAT from the castration + TP group compared to the control group.

In WAT from the HFD group, the Ar mRNA and protein levels are very low to undetectable (data now shown).

Thus, castration results in the reduced expression of Ar in WAT on both mRNA and protein levels. Ar mRNA and protein is not detectable in WAT from animals fed HFD.

4. Discussion

Our data demonstrate that surgical castration has profound effects on WAT. The WAT wet weight and the WAT wet weight/body weight ratio were lower in the castration + TP group and reached statistical significance in the regular-diet group. These results suggest that testosterone does not fully abrogate effects of castration in the regular-diet group. Morphologic changes after castration were associated with adipocyte size reduction, an increase in a stromal compartment, and macrophage infiltration.

Our data further indicate that lipolytic enzymes can be activated in a sustained fashion in response to castration, as observed in the HFD group. We also detected increased Atgl protein levels in the HFD group after castration. Our data further indicate that animals in the HFD group respond differently to the castration stimulus than animals in the regular-diet group, potentially as a consequence of a more robust and/or sustained lipolytic program.

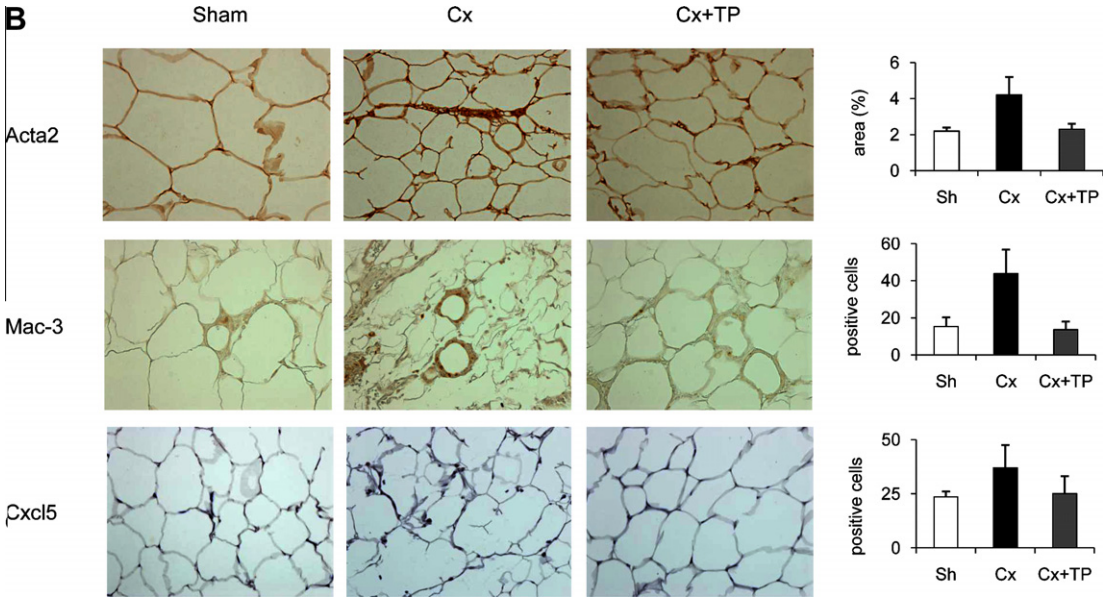

Fig. 4 (*continued*)

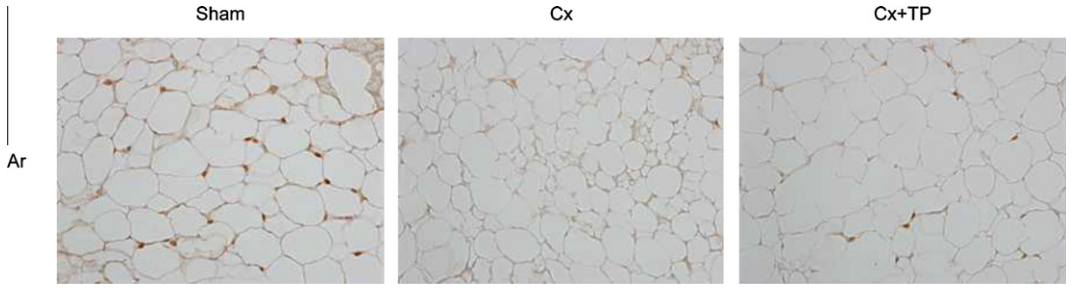

Fig. 5. Immunohistochemical staining for androgen receptor (Ar) of paraffin-embedded WAT from mice fed a regular diet. Antibodies against Ar were used as described in Section 2. Images were depicted at 20× magnification. Sh, sham-operated; Cx, castration; Cx + TP, castration + testosterone pellet.

In our view, these data further suggest that the lipolytic process does not continue indefinitely and may subside at a certain set-point. It may take longer for the HFD group to reach such set-point as lipolysis is still ongoing 14 days after castration. Future studies that analyze $pHsl^{Ser660}$ and Atgl protein levels at different time points after castration under various conditions may clarify this hypothesis.

Serum leptin levels were reduced in both dietary groups after castration, whereas serum resistin and adiponectin levels were increased in the regular-diet group after castration. Serum resistin and adiponectin levels were not affected by castration in the HFD group. Inoue et al. (2010) reported increased plasma adiponectin levels in castrated C57BL/6 mice independent of diet, and decreased plasma leptin levels in castrated mice on high carbohydrate diet. Xu et al. (2005) measured increased serum adiponectin levels in castrated C57BL/6 mice.

Controls in the HFD group had higher body weight, the WAT wet weight/body weight ratio and BMI than the controls in regular-diet group at the time of sacrifice (Fig. 2S, Supplementary data). We also measured serum glucose and triglyceride (TG) levels. Our data demonstrate that castration has a small but significant effect in the regular diet group and a profound effect on serum TG levels in the HFD group. This effect was modified but not offset by testosterone replacement. Serum glucose levels were also affected only in the HFD group by castration and testosterone did not offset the castration effect. Our results suggest that castration alters the mechanism(s) regulating serum TG and glucose levels, selectively in the HFD group. The physiological mechanisms responsible for these metabolic changes need further investigation.

In addition to leptin, adiponectin, and resistin, adipose tissue expresses a wide range of factors, including pro-inflammatory cytokines and chemokines. The expression of IL-8, MCP-1/CCL2, and macrophage inflammatory protein is increased with adipocity in animals and humans (Sengenes et al., 2007). We detected *Cxcl5*, *Cxcl2*, and *Il4* in the regular-diet group and *Cxcl5*, *Il1a*, and *Mmp2* in the high-fat-diet group among the most induced cytokines after castration. The mRNA levels of *Cxcl1*, *Ccl7*, *Ccl2*, *Cxcl2*, *Tnf,* and *Ccl3* were higher in the control WAT from the HFD group than they were in the control regular-diet group. Chemokines and their corresponding receptors, including CCL2, CCL5, CXCL5, CXCL13, CXCL16, and CXCR5, have been shown to be involved in prostate cancer progression and organ-specific metastasis (Loberg et al., 2006; Sung et al., 2008; Singh et al., 2009). Further studies are needed to characterize cytokine-producing cells types in WAT.

We hypothesized that increased presence of stromal cells may be a result of the tissue regeneration process induced in WAT by castration. We detected increased Fasn staining in the stromal compartment of WAT from castrated mice, suggesting that the stromal compartment is involved in WAT remodeling after castration. Fasn is highly expressed in differentiating mouse 3T3-L1 preadipocytes (Paulauskis and Sul, 1988).

Interestingly, few cells within the stromal compartment in WAT from the castration + TP regular-diet group stained for Fasn. This suggests that testosterone may inhibit differentiation of stromal pre-adipocytes. It was reported that testosterone inhibits adipogenic differentiation of mouse 3T3-L1 pre-adipocytes (Singh et al., 2006).

It has been suggested that macrophages present in non inflamed tissue (i.e., resident macrophages) help maintain homeostasis and participate in tissue remodeling. In mice, these cells originate from circulating $CCR2^{-}CX3CR1^{hi}$ monocytes. In contrast, $CCR2^{+}CX3CR1^{low}$ monocytes migrate into inflamed tissue and differentiate into macrophages, which coordinate inflammatory responses by producing chemokines and clearing debris by phagocytosis (Lumeng et al., 2007). Future studies may explain the origin and provide an expression profile of macrophages that are found in WAT after castration.

Dieudonne et al. (1998) documented that human and rat pre-adipocytes and adipocytes express androgen receptor and suggested that androgens may contribute, through regulation of their own receptors, to the control of adipose tissue development. Yu et al. (2008) generated adipose-specific Ar knockout mice by a conditional genetic knockout approach. Dhindsa et al. (2010) reported that obesity is probably the condition most frequently associated with subnormal free testosterone concentrations in males. Our analysis confirmed the expression of Ar in epididymal WAT from mice fed regular diet and that the consumption of high-fat diet may result in the reduction of the Ar expression and reduced serum testosterone levels. Kyprianou and Isaacs, (1988) demonstrated that castration induced a series of temporally discrete biochemical events, including rapid loss of nuclear Ar and programmed cell death, within the rat ventral prostate. We detected the loss of nuclear Ar in WAT after castration but no apparent apoptosis (data not shown). Thus, mechanisms leading to reduced Ar levels at the time points analyzed in WAT after castration ought to be further studied.

Complex short-term effects of castration in rodents have not been studied in great detail. Published studies focus on long-term effects of castration (Koncarevic et al., 2010; Axell et al., 2006; Hastings and Hill, 1997; Vanderschueren et al., 2004) which are relevant to men undergoing androgen deprivation therapy. We hypothesize that we fortuitously selected a time point at which biochemical events which contribute to the effects of long-term androgen deprivation therapy in WAT are initiated.

In conclusion, our study demonstrated that castration has profound effects on mouse epididymal WAT. Future studies involving human WAT are needed to understand underlying biologic mechanisms during castration and to test the clinical relevance of these findings to the management of obesity, metabolic syndrome, and prostate cancer in humans.

Grants

This research is supported in part by the NIH grant R01CA050588, the DOD grant PC093932, and in part by the NIH through MD Anderson's Cancer Center Support Grant, CA016672.

Conflict of interest statement

None of the authors have any conflict of interest to declare.

Acknowledgements

The authors thank Karen F. Phillips, ELS, from the Department of Genitourinary Medical Oncology, MD Anderson Cancer Center, for editorial assistance.

Appendix A. Supplementary data

Supplementary data associated with this article can be found, in the online version, at doi:10.1016/j.mce.2011.07.011.

References

Axell, A.M., MacLean, H.E., Plant, D.R., Harcourt, L.J., Davis, J.A., Jimenez, M., Handelsman, D.J., Lynch, G.S., Zajac, J.D., 2006. Continuous testosterone administration prevents skeletal muscle atrophy and enhances resistance to fatigue in orchidectomized male mice. Am. J. Physiol. Endocrinol. Metab. 291, E506–E516.

Bain, J., 2010. Testosterone and the aging male: to treat or not to treat? Maturitas 66, 16–22.

Catenacci, V.A., Hill, J.O., Wyatt, H.R., 2009. The obesity epidemic. Clin. Chest. Med. 30, 415–444, vii.

Chu, Y., Huddleston, G.G., Clancy, A.N., Harris, R.B., Bartness, T.J., 2010. Epididymal fat is necessary for spermatogenesis, but not testosterone production or copulatory behavior. Endocrinology 151, 5669–5679.

Collins, S., Martin, T.L., Surwit, R.S., Robidoux, J., 2004. Genetic vulnerability to diet-induced obesity in the C57BL/6J mouse: physiological and molecular characteristics. Physiol. Behav. 81, 243–248.

Dhindsa, S., Miller, M.G., McWhirter, C.L., Mager, D.E., Ghanim, H., Chaudhuri, A., Dandona, P., 2010. Testosterone concentrations in diabetic and nondiabetic obese men. Diabetes Care 33, 1186–1192.

Dieudonne, M.N., Pecquery, R., Boumediene, A., Leneveu, M.C., Giudicelli, Y., 1998. Androgen receptors in human preadipocytes and adipocytes: regional specificities and regulation by sex steroids. Am. J. Physiol. 274, C1645–52.

Fair, A.M., Montgomery, K., 2009. Energy balance, physical activity, and cancer risk. Methods Mol. Biol. 472, 57–88.

Fruhbeck, G., 2008. Overview of adipose tissue and its role in obesity and metabolic disorders. Methods Mol. Biol. 456, 1–22.

Galic, S., Oakhill, J.S., Steinberg, G.R., 2010. Adipose tissue as an endocrine organ. Mol. Cell Endocrinol. 316, 129–139.

Hansel, W., 2010. The essentiality of the epididymal fat pad for spermatogenesis. Endocrinology 151, 5565–5567.

Hastings, I.M., Hill, W.G., 1997. The effect of testosterone in mice divergently selected on fat content or body weight. Genet. Res. 70, 135–141.

Inoue, T., Zakikhani, M., David, S., Algire, C., Blouin, M.J., Pollak, M., 2010. Effects of castration on insulin levels and glucose tolerance in the mouse differ from those in man. Prostate 70, 1628–1635.

Koncarevic, A., Cornwall-Brady, M., Pullen, A., Davies, M., Sako, D., Liu, J., Kumar, R., Tomkinson, K., Baker, T., Umiker, B., Monnell, T., Grinberg, A.V., Liharska, K., Underwood, K.W., Ucran, J.A., Howard, E., Barberio, J., Spaits, M., Pearsall, S., Seehra, J., Lachey, J., 2010. A soluble activin receptor type IIb prevents the effects of androgen deprivation on body composition and bone health. Endocrinology 151, 4289–4300.

Kyprianou, N., Isaacs, J.T., 1988. Activation of programmed cell death in the rat ventral prostate after castration. Endocrinology 122, 552–562.

Loberg, R.D., Day, L.L., Harwood, J., Ying, C., St John, L.N., Giles, R., Neeley, C.K., Pienta, K.J., 2006. CCL2 is a potent regulator of prostate cancer cell migration and proliferation. Neoplasia 8, 578–586.

Lumeng, C.N., Deyoung, S.M., Bodzin, J.L., Saltiel, A.R., 2007. Increased inflammatory properties of adipose tissue macrophages recruited during diet-induced obesity. Diabetes 56, 16–23.

Paulauskis, J.D., Sul, H.S., 1988. Cloning and expression of mouse fatty acid synthase and other specific mRNAs: developmental and hormonal regulation in 3T3-L1 cells. J. Biol. Chem. 263, 7049–7054.

Roberts, D.L., Dive, C., Renehan, A.G., 2010. Biological mechanisms linking obesity and cancer risk: new perspectives. Annu. Rev. Med. 61, 301–316.

Sengenes, C., Miranville, A., Lolmede, K., Curat, C.A., Bouloumie, A., 2007. The role of endothelial cells in inflamed adipose tissue. J. Intern. Med. 262, 415–421.

Singh, R., Artaza, J.N., Taylor, W.E., Braga, M., Yuan, X., Gonzalez-Cadavid, N.F., Bhasin, S., 2006. Testosterone inhibits adipogenic differentiation in 3T3-L1 cells: nuclear translocation of androgen receptor complex with beta-catenin and T-cell factor 4 may bypass canonical Wnt signaling to down-regulate adipogenic transcription factors. Endocrinology 147, 141–154.

Singh, S., Singh, R., Sharma, P.K., Singh, U.P., Rai, S.N., Chung, L.W., Cooper, C.R., Novakovic, K.R., Grizzle, W.E., Lillard Jr., J.W., 2009. Serum CXCL13 positively correlates with prostatic disease, prostate-specific antigen and mediates prostate cancer cell invasion, integrin clustering and cell adhesion. Cancer Lett. 283, 29–35.

Spandidos, A., Wang, X., Wang, H., Seed, B., 2010. PrimerBank: a resource of human and mouse PCR primer pairs for gene expression detection and quantification. Nucleic Acids Res. 38, D792–9.

Sung, S.Y., Hsieh, C.L., Law, A., Zhau, H.E., Pathak, S., Multani, A.S., Lim, S., Coleman, I.M., Wu, L.C., Figg, W.D., Dahut, W.L., Nelson, P., Lee, J.K., Amin, M.B., Lyles, R., Johnstone, P.A., Marshall, F.F., Chung, L.W., 2008. Coevolution of prostate cancer and bone stroma in three-dimensional coculture: implications for cancer growth and metastasis. Cancer Res. 68, 9996–10003.

Tran, T.T., Kahn, C.R., 2010. Transplantation of adipose tissue and stem cells: role in metabolism and disease. Nat. Rev. Endocrinol. 6, 195–213.

Vanderschueren, D., Vandenput, L., Boonen, S., Lindberg, M.K., Bouillon, R., Ohlsson, C., 2004. Androgens and bone. Endocr. Rev. 25, 389–425.

Xu, A., Chan, K.W., Hoo, R.L., Wang, Y., Tan, K.C., Zhang, J., Chen, B., Lam, M.C., Tse, C., Cooper, G.J., Lam, K.S., 2005. Testosterone selectively reduces the high molecular weight form of adiponectin by inhibiting its secretion from adipocytes. J. Biol. Chem. 280, 18073–18080.

Yu, I.C., Lin, H.Y., Liu, N.C., Wang, R.S., Sparks, J.D., Yeh, S., Chang, C., 2008. Hyperleptinemia without obesity in male mice lacking androgen receptor in adipose tissue. Endocrinology 149, 2361–2368.

Zhang, Y., Daquinag, A., Traktuev, D.O., Amaya-Manzanares, F., Simmons, P.J., March, K.L., Pasqualini, R., Arap, W., Kolonin, M.G., 2009. White adipose tissue cells are recruited by experimental tumors and promote cancer progression in mouse models. Cancer Res. 69, 5259–5266.